

Open-Framework Oxysulfide Based on the Supertetrahedral $[\text{In}_4\text{Sn}_{16}\text{O}_{10}\text{S}_{34}]^{12-}$ Cluster and Efficient Sequestration of Heavy Metals

Xian-Ming Zhang,^{*,†,||} Debajit Sarma,^{§,||} Ya-Qin Wu,[†] Li Wang,^{*,‡,§} Zhi-Xue Ning,[†] Fu-Qiang Zhang,[†] and Mercouri G. Kanatzidis^{*,§}

[†]School of Chemistry and Material Science, Shanxi Normal University Linfen 041004, P. R. China

[‡]College of Chemistry and Chemical Engineering, Xinjiang Normal University, Urumqi 830054, P. R. China

[§]Department of Chemistry, Northwestern University, Evanston, Illinois 60208, United States

Supporting Information

ABSTRACT: The new ion-exchange oxy-sulfide material has a three-dimensional open framework comprising the pseudo-T4 supertetrahedral $[\text{In}_4\text{Sn}_{16}\text{O}_{10}\text{S}_{34}]^{12-}$ cluster. This material has large pores and is a fast ion exchanger. It exhibits high selectivity in sequestering heavy metal ions from aqueous solutions including solutions containing heavy concentrations of sodium, calcium, ammonium, magnesium, zinc, carbonate, phosphate, and acetate ions. Moreover, the ion-exchange efficiency in competitive ion-exchange experiments involving mixtures of metal ions is significantly higher than for solutions of single metal ions.

The effective remediation of heavy metal ions (Cd^{2+} , Hg^{2+} , and Pb^{2+}) is a great challenge as they present a major hazard as potent environmental pollutants to living beings in drinking and wastewater.¹ In this regard, a wide variety of stable inorganic oxide materials such as, zeolites, clays and functionalized clays, activated carbon, organoceramics, mesoporous silica as well as recently developed metal-organic frameworks have been tested for removal of these ions from wastewater.² Since original recognition,³ crystalline chalcogenide open frameworks, which often show distinct supertetrahedral clusters based structural features,^{4–7} have attracted great attention because these materials are capable of integrating porosity, semiconductor related properties, and photocatalysis.⁸ Over the past decade, crystalline chalcogenide families have emerged as highly promising candidates for removal of heavy ions from wastewater. The selectivity of the chalcogenide family arises from affinity of their soft basic frameworks for soft Lewis acids (e.g., Cd^{2+} , Hg^{2+} , and Pb^{2+}).⁹ The chalcogenides $(\text{NH}_4)_2\text{In}_4\text{Se}_{20}$, $\text{K}_{2x}\text{M}_x\text{Sn}_{3-x}\text{S}_6$ (KMS-1 and KMS-2) have been reported to show excellent heavy metal ion absorption properties.¹⁰ We expect that the incorporation of oxygen atoms in sulfide networks will create oxysulfide open-framework materials that can combine the excellent affinity to heavy metals of chalcogenide materials and good stability of oxide materials.¹¹ To date, this kind of oxysulfide open-framework material has been little explored even though it promises unique applications.¹² Herein we report a new oxysulfide with a three-dimensional open framework of $[\text{In}_4\text{Sn}_{16}\text{O}_{10}\text{S}_{32}]^{8-}$ based on the pseudo-T4 $[\text{In}_4\text{Sn}_{16}\text{O}_{10}\text{S}_{34}]^{12-}$ cluster. This material shows good stability attributed to the incorporation of oxygen

atoms into the sulfide network and facile ion-exchange properties with strong selectivity for heavy metal ions. This high performance is due to the strong bonding affinity of the sulfur atoms in the framework for heavy metal ions.

The reaction¹³ of $\text{SnCl}_2 \cdot 2\text{H}_2\text{O}$, $\text{In}(\text{NO}_3)_3$, S, 1,3-di(4-pyridyl)propane (dpp), and ethanolamine (eta) in water at 160 °C generated pale-yellow octahedral crystals of **1**, and the empirical formula was established with elemental analysis (CHN, flame atom adsorption spectroscopy, and energy dispersive spectroscopy (EDS)), thermal gravimetric analysis, infrared (IR) spectroscopy (see SI experimental section, Tables S1, S2, and Figures S1, S2).

The crystal structure was solved and refined with single crystal X-ray diffraction (XRD) analysis¹⁴ which revealed a novel oxysulfide pseudo-T4 $[\text{In}_4\text{Sn}_{16}\text{O}_{10}\text{S}_{34}]^{12-}$ cluster and established the open-framework nature of **1**. The new material crystallizes in the tetragonal space group $I4_1/acd$, and the asymmetric unit contains five crystallographically independent M atoms, three O atoms, and nine S atoms as shown in Figure S3. There are three types of metal sites in the $[\text{In}_4\text{Sn}_{16}\text{O}_{10}\text{S}_{34}]^{12-}$ cluster. The In(1) site shows a distorted octahedral InO_3S_3 geometry being coordinated by three sulfur atoms and three oxygen atoms. The Sn(1), Sn(2)m and Sn(3) sites also show distorted octahedral geometries but are coordinated by four sulfur atoms and two oxygen atoms. These have two short Sn–S bonds, two long Sn–S bonds, one short Sn–O bond, and one long Sn–O bond. The bond lengths and valence bond sum analyses suggest that the three metal sites are Sn(IV) sites.¹⁵ The basic building unit in **1** is the pseudo-T4 $[\text{In}_4\text{Sn}_{16}\text{O}_{10}\text{S}_{34}]^{12-}$ cluster (Figure 1a), which is composed of 4 corner and edge-shared SnS_4 tetrahedra, 12 SnS_4O_2 octahedra, and 4 InS_3O_3 octahedra.

According to Pauling's electrostatic valence rule or Brown's equal valence rule, ideal T4 and even larger supertetrahedral clusters will be unstable for trivalent and tetravalent cations.¹⁶ Here, nature selects the absence of μ_4 -sulfide atom and insertion of oxygen anions to avoid excessively high charge at the μ_3 -sulfur sites in **1**. The missing of metal core has been observed in supertetrahedral chalcogenide clusters,^{4b} but the missing of sulfur core and the presence of 10 oxygen atoms in a pseudo-T4 cluster to our knowledge has not been reported

Received: March 21, 2016

Published: April 15, 2016

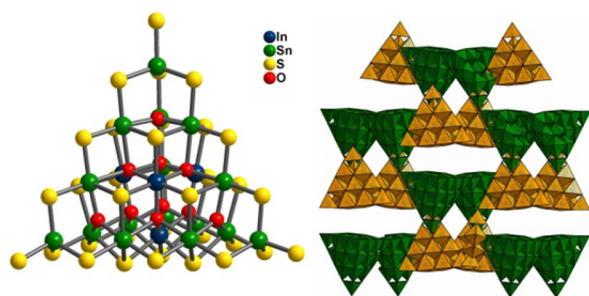
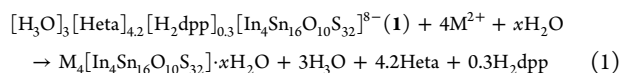


Figure 1. (a) The pseudo-T4 supertetrahedral $[\text{In}_4\text{Sn}_{16}\text{O}_{10}\text{S}_{34}]^{12-}$ cluster (left) and (b) 3D two-fold interpenetrated framework along the $[111]$ direction (right). Note: Each cluster uses four corner-shared S atoms to bind with its four neighbors to form the anionic framework of $[\text{In}_4\text{Sn}_{16}\text{O}_{10}\text{S}_{32}]^{8-}$.

previously. In other words, the 34 sulfur atoms in the pseudo-T4 cluster are cubic close-packed but have a vacancy at the center. Among the 10 oxygen atoms in the pseudo-T4 cluster, there are 6 μ_4 and 4 μ_3 oxygen atoms as shown in Figures S4 and S5. Although T2 $[\text{Sn}_4\text{Se}_{10}\text{O}]^{6-}$ and T3 $[\text{Sn}_{10}\text{S}_{20}\text{O}_4]^{8-}$ oxychalcogenide clusters and their open frameworks have been synthesized,¹² no T4 oxychalcogenide cluster appears to have been documented to date.

The pseudo-T4 $[\text{In}_4\text{Sn}_{16}\text{O}_{10}\text{S}_{34}]^{12-}$ clusters share corners to form a 3D topological cristobalite open-framework structure with formula $[\text{In}_4\text{Sn}_{16}\text{O}_{10}\text{S}_{32}]^{8-}$ (Figure 1b). Each pseudo-T4 tetrahedron is nearly regular with edge lengths of 14.8 and 15.0 Å. Despite being two-fold interpenetrated, compound **1** contains large cavities. As can be seen, there are 20×6 Å² rectangular channels along the $[111]$ projection. Although the positions of the framework atoms were determined accurately, the organic cations and water molecules filling the pores were not located because of the positional disorder typically encountered in this kind of structure.

To check the feasibility of ion exchange of the organic cations, we immersed compound **1** in a solution of M^{2+} ($\text{M}^{2+} = \text{Cd}^{2+}$, Hg^{2+} , and Pb^{2+}) ions for 15 h. The ion-exchange processes are generally very rapid, but to ensure a complete ion exchange, it was run for 15 h. The EDS of the exchanged materials showed the presence of Cd^{2+} , Hg^{2+} , and Pb^{2+} ions (Figure S6). The PXRD of the exchanged materials showed isotactic ion exchange with retention of the parent structure (Figure S7). Compared with as-synthesized **1**, the C and N fraction in elemental analyses is strongly decreased, largely consistent with heavy metal ion exchange (Table S3). The ion-exchange processes can be described by the following equation:



The water molecules present inside the channels of compound **1** during ion exchange confirmed by TG analyses of ion-exchanged samples (Figure S8). We also find that in the absence of the soft metal ions, the compound undergoes facile ions exchange with Cs^+ ions (~80% of the organic cations can be exchanged as confirmed by EDS).

The Cd^{2+} , Hg^{2+} , and Pb^{2+} ion exchange results are presented in Figure 2. The ion exchange of **1** using a 10 ppm solutions of Cd^{2+} , Hg^{2+} , and Pb^{2+} shows that ~58% (Cd^{2+}), 74% (Hg^{2+}), and 65% (Pb^{2+}) of the ions were removed from the solution. However, the ion exchange increases dramatically in the presence of high salt concentration (NaCl, CaCl_2). For

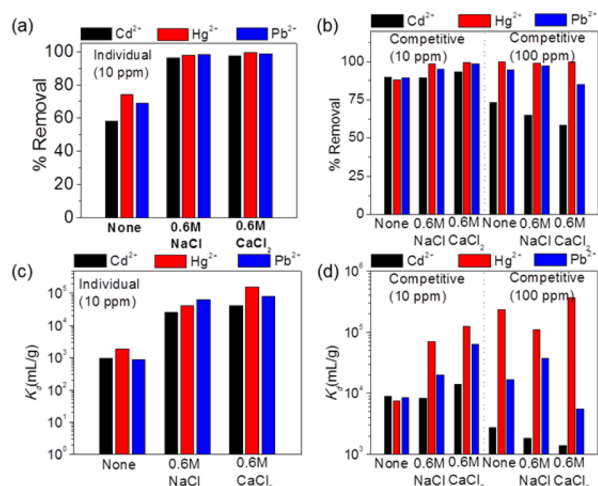


Figure 2. Plot of % removal of heavy metal ions (Cd^{2+} , Hg^{2+} , and Pb^{2+}) from solution: (a) individual ion-exchange and (b) competitive ion-exchange experiments. The variation of the distribution coefficient K_d for (c) individual and (d) competitive Cd^{2+} , Hg^{2+} , and Pb^{2+} ion-exchange experiments.

example, the ion exchanged in 0.6 M NaCl increases to ~96 (Cd^{2+}), 97 (Hg^{2+}), and 98 (Pb^{2+})%, whereas, in case of 0.6 M CaCl_2 , it increases to ~97 (Cd^{2+}), 99 (Hg^{2+}), and 98 (Pb^{2+})%. This increase in ion exchange is possibly due to the fact that mass action from the very high concentration of Na^+ and Ca^{2+} ions (compared to the heavy metal ions) causes the alkaline ions to enter into pores of **1** first to exchange with organic cations (kinetic control). However, the kinetically faster exchanging Na^+ and Ca^{2+} ions are then exchanged out by heavy metal ions because Cd^{2+} , Hg^{2+} , and Pb^{2+} (softer Lewis acids) ions show stronger bonding interaction with the soft basic (S^{2-}) sites (thermodynamic control). We assume the organic cations are held inside the cavities more strongly since they have served as templates for the assembly of the 3D framework, whereas the hydrated Na^+ and Ca^{2+} ions are not.

A competitive ion-exchange experiment using solutions containing mixtures of Cd^{2+} , Hg^{2+} , and Pb^{2+} ions of ~10 ppm (each) showed that the ion-exchange efficiency increases to ~89 (Cd^{2+}), 88 (Hg^{2+}), and 89 (Pb^{2+})%, which also can be contributed to the overall increase of the ionic strength of the solution. The competitive ion exchange is enhanced in the presence of excess NaCl (~89% Cd^{2+} , 98% Hg^{2+} , and 95% Pb^{2+}) or excess CaCl_2 (~93% Cd^{2+} , 99% Hg^{2+} , and 99% Pb^{2+}). The preference of **1** for the ions was not clear from the ~10 ppm solution as it captured almost all the ions. To get a clear distinction of the relative preferences of **1** for these ions, we performed the same competitive ion-exchange experiments with ~100 ppm (each), which showed that ~73 (Cd^{2+}), 99 (Hg^{2+}), and 94 (Pb^{2+}) % of the ions are exchanged from the solution. The preference of **1** follows the order $\text{Cd}^{2+} < \text{Pb}^{2+} < \text{Hg}^{2+}$. The distribution coefficient K_d values were found to be 0.9×10^3 to 4.0×10^4 mL/g for Cd^{2+} , 1.8×10^3 to 1.5×10^5 mL/g for Hg^{2+} , and 0.9×10^3 to 7.8×10^4 mL/g for Pb^{2+} , which indicate that **1** is considered to be very good material for ion exchange. Competitive ion-exchange experiments using solutions containing mixtures of Cd^{2+} , Hg^{2+} , and Pb^{2+} ions of ~10 ppm (each) in 0.6 M NH_4NO_3 , $\text{Mg}(\text{NO}_3)_2$, $\text{Zn}(\text{NO}_3)_2$, Na_2CO_3 , Na_3PO_4 , and CH_3COONa solution showed that the ion-exchange efficiencies are in the range of 91–97 (Cd^{2+}), 94–99 (Hg^{2+}), and 89–99 (Pb^{2+})% (Figure S10). The effect of

pH on the removal of heavy metal ions showed ion-exchange efficiency of 97–99 (Cd^{2+}), 98–99 (Hg^{2+}), and 92–96 (Pb^{2+})% at $\text{pH} \sim 2$ –10, however at $\text{pH} = 12$ we observed a significant decrease in ion exchange efficiency (Figure S11).

To evaluate the preferred binding sites in the framework for the incoming heavy metal ions, we simply estimated the binding energy (BE)¹⁷ between the absorbed $\text{M}(\text{H}_2\text{O})_6^{2+}$ and a model $[\text{In}_4\text{Sn}_{16}\text{O}_{10}\text{S}_{34}\text{H}_4]^{8-}$ cluster based on the $[\text{M}(\text{H}_2\text{O})_6]^{2+}$ $[\text{In}_4\text{Sn}_{16}\text{O}_{10}\text{S}_{34}\text{H}_4]$ ($\text{M} = \text{Mg}, \text{Ca}, \text{Cd}, \text{Hg}$) unit (Figure 3). In

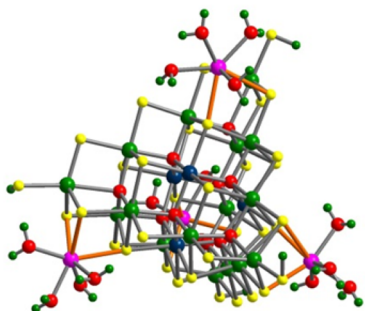


Figure 3. Simulated binding sites in the $[\text{In}_4\text{Sn}_{16}\text{O}_{10}\text{S}_{34}\text{H}_4]^{8-}$ cluster to heavy metal ions (Cd^{2+} , Hg^{2+} , purple balls). Note: Water molecules (red balls) are also involved in model structure.

our model, four H atoms were added to terminal S and four $[\text{M}(\text{H}_2\text{O})_6]^{2+}$ complexes were absorbed to keep the charge neutrality of the overall structure. Overall, the total BE can be considered a measure of the interaction between the adsorbate and framework model structure. In the optimized structure, each heavy metal ion is chelated as $\text{M}(\text{H}_2\text{O})_3^{2+}$ by three sulfur atoms from the model framework structure. Among the three components that contribute to BE (Table S4), the Pauli repulsion contribution acting as a destabilization term is reflected in the larger energy shift of the antibonding orbitals relative to bonding orbitals, whereas the electrostatic interaction (EI) and orbital interaction (OI) contributions are stabilizing in nature. The EI is dominated by the electrostatic coulomb attractions, and OI arises from the M–S bonding through the mixing of occupied and unoccupied orbitals sulfur and metal orbitals, respectively. As can be seen in Table S4, the calculated BE exhibits a clear trend of $\text{Ca}^{2+} < \text{Cd}^{2+} < \text{Hg}^{2+}$, in which the heavy metal ions are favored over the alkaline earth atom, in good agreement with our experiments.

In contrast to the previously reported supertetrahedral chalcogenide clusters and their open frameworks, the incorporation of oxygen gives new clusters and allows for a different construction principle. Specifically, the coordination polyhedra of the metals in the oxysulfide clusters are no longer limited to tetrahedra. This revelation offers a path to a rich set of stable new oxychalcogenide clusters and open frameworks. The large continuous void space in compound **1** favors the fast movement of counterions in and out of the structure. Because of the selective bonding interactions of the soft Lewis basic (S^{2-}) sites to heavy metal ions, this material selectively sequesters heavy metal ions from aqueous solutions including ones with heavy concentrations of sodium, calcium, ammonium, magnesium, zinc, carbonate, phosphate, and acetate ions. In contrast to chalcogenide clusters, oxychalcogenide clusters can increase the stability of large clusters due to incorporation of O anions. We expect that the incorporation of more oxygen atoms in sulfide networks will create oxysulfide open-frame-

work materials that can combine the semiconductor properties of chalcogenide materials and good stability of oxide materials.

■ ASSOCIATED CONTENT

Supporting Information

The Supporting Information is available free of charge on the ACS Publications website at DOI: 10.1021/jacs.6b02959.

Experimental details and data (PDF)

Crystal structural data (CIF)

■ AUTHOR INFORMATION

Corresponding Authors

*zhangxm@dns.sxnu.edu.cn

*wangliresearch@163.com

*m-kanatzidis@northwestern.edu

Author Contributions

^{||}Xian-Ming Zhang and Debajit Sarma contributed equally.

Notes

The authors declare no competing financial interest.

■ ACKNOWLEDGMENTS

This work was financially supported by 10,000 Talent Plan, NSFC (2095101, 21371147, 21365021), the Ministry of Education of China (no. IRT1156), and XJOYF (grant no. 2013711009). At Northwestern this research was supported by the National Science Foundation (Grant DMR-1410169).

■ REFERENCES

- (1) (a) *Ten chemicals of major public health concern*; WHO: Geneva, http://www.who.int/ipcs/assessment/public_health/chemicals_phc/en/. (b) Clarkson, T. W. *Heavy metals in the environment*; Sarkar, B., Ed.; Marcel Dekker, New York, 2002; p 457. (c) Shannon, M. A.; Bohn, P. W.; Elimelech, M.; Georgiadis, J. G.; Marinas, B. J.; Mayes, A. M. *Nature* **2008**, *452*, 301–310. (d) Schwarzenbach, R. P.; Escher, B. I.; Fenner, K.; Hofstetter, T. B.; Johnson, C. A.; von Gunten, U.; Wehrli, B. *Science* **2006**, *313*, 1072.
- (2) (a) Mercier, L.; Pinnavaia, T. J. *Adv. Mater.* **1997**, *9*, 500–503. (b) Feng, X.; Fryxell, G. E.; Wang, L. Q.; Kim, A. Y.; Liu, J.; Kemner, K. M. *Science* **1997**, *276*, 923. (c) Brown, J.; Mercier, L.; Pinnavaia, T. J. *Chem. Commun.* **1999**, 69–70. (d) Lagadic, I. L.; Mitchell, M. K.; Payne, B. D. *Environ. Sci. Technol.* **2001**, *35*, 984–990. (e) Shin, Y. S.; Fryxell, G.; Um, W. Y.; Parker, K.; Mattigod, S. V.; Skaggs, R. *Adv. Funct. Mater.* **2007**, *17*, 2897–2901. (f) Chakraborty, A.; Bhattacharyya, S.; Hazra, A.; Ghosh, A. C.; Maji, T. K. *Chem. Commun.* **2016**, *52*, 2831–2834. (g) Abney, C. W.; Gilhula, J. C.; Lu, K.; Lin, W. *Adv. Mater.* **2014**, *26*, 7993–7997. (h) Ke, F.; Qiu, L. G.; Yuan, Y. P.; Peng, F. M.; Jiang, X.; Xie, A. J.; Shen, Y. H.; Zhu, J. F. *J. Hazard. Mater.* **2011**, *196*, 36–43.
- (3) (a) Bedard, R. L.; Vail, L. D.; Wilson, S. T.; Flanigen, E. M. U.S. Patent 4880761, November 14, 1989. (b) Yaghi, O. M.; Sun, Z.; Richardson, D. A.; Groy, T. L. *J. Am. Chem. Soc.* **1994**, *116*, 807–808.
- (4) (a) Wang, L.; Wu, T.; Zuo, F.; Zhao, X.; Bu, X.; Wu, J.; Feng, P. *J. Am. Chem. Soc.* **2010**, *132*, 3283–3285. (b) Wang, C.; Bu, X.; Zheng, N.; Feng, P. *J. Am. Chem. Soc.* **2002**, *124*, 10268–10269.
- (5) (a) Manos, M. J.; Chrissafis, K.; Kanatzidis, M. G. *J. Am. Chem. Soc.* **2006**, *128*, 8875–8883. (b) Ding, N.; Chung, D.-Y.; Kanatzidis, M. G. *Chem. Commun.* **2004**, 1170–1171. (c) Wu, T.; Wang, X.; Bu, X.; Zhao, X.; Wang, L.; Feng, P. *Angew. Chem., Int. Ed.* **2009**, *48*, 7204–7207. (d) Bag, S.; Kanatzidis, M. G. *J. Am. Chem. Soc.* **2010**, *132*, 14951–14959. (e) Li, J. R.; Xie, Z. L.; He, X. W.; Li, L. H.; Huang, X. Y. *Angew. Chem., Int. Ed.* **2011**, *50*, 11395–11399.
- (6) Zheng, N.; Bu, X.; Feng, P. *J. Am. Chem. Soc.* **2005**, *127*, 5286–5287.

(7) (a) Parise, J. B.; Ko, Y. *Chem. Mater.* **1994**, *6*, 718–720. (b) Ahari, H.; Lough, A.; Petrov, S.; Ozin, G. A.; Bedard, R. L. *J. Mater. Chem.* **1999**, *9*, 1263.

(8) (a) Mroczek, A.; Kanatzidis, M. G. *Acc. Chem. Res.* **2003**, *36*, 111. (b) Feng, P.; Bu, X.; Zheng, N. *Acc. Chem. Res.* **2005**, *38*, 293. (c) Li, H.; Laine, A.; O'Keeffe, M.; Yaghi, O. M. *Science* **1999**, *283*, 1145. (d) Rangan, K. K.; Trikalitis, P. N.; Kanatzidis, M. G. *J. Am. Chem. Soc.* **2000**, *122*, 10230. (e) Huang, X.; Heulings, H. R., IV; Le, V.; Li, J. *Chem. Mater.* **2001**, *13*, 3754. (f) Manos, M. J.; Iyer, R. G.; Quarez, E.; Liao, J. H.; Kanatzidis, M. G. *Angew. Chem., Int. Ed.* **2005**, *44*, 3552. (g) Feng, M. L.; Kong, D. N.; Xie, Z. L.; Huang, X. Y. *Angew. Chem., Int. Ed.* **2008**, *47*, 8623–8626.

(9) (a) Subrahmanyam, K. S.; Malliakas, C. D.; Sarma, D.; Armatas, G. S.; Wu, J.; Kanatzidis, M. G. *J. Am. Chem. Soc.* **2015**, *137*, 13943–13948. (b) Subrahmanyam, K. S.; Sarma, D.; Malliakas, C. D.; Polychronopoulou, K.; Riley, B. J.; Pierce, D. A.; Chun, J.; Kanatzidis, M. G. *Chem. Mater.* **2015**, *27*, 2619–2626. (c) Bag, S.; Trikalitis, P. N.; Chupas, P. J.; Armatas, G. S.; Kanatzidis, M. G. *Science* **2007**, *317*, 490–493.

(10) (a) Manos, M. J.; Malliakas, C. D.; Kanatzidis, M. G. *Chem. - Eur. J.* **2007**, *13*, 51. (b) Manos, M. J.; Kanatzidis, M. G. *Chem. - Eur. J.* **2009**, *15*, 4779–4784. (c) Fard, Z. H.; Malliakas, C. D.; Mertz, J. L.; Kanatzidis, M. G. *Chem. Mater.* **2015**, *27*, 1925. (d) Ma, S.; Chen, Q.; Li, H.; Wang, P.; Islam, S. M.; Gu, Q.; Yang, X.; Kanatzidis, M. G. *J. Mater. Chem. A* **2014**, *2*, 10280. (e) Mertz, J. L.; Fard, Z. H.; Malliakas, C. D.; Manos, M. J.; Kanatzidis, M. G. *Chem. Mater.* **2013**, *25*, 2116.

(11) (a) Davis, M. E. *Nature* **2002**, *417*, 813. (b) Zou, X.; Conradsson, T.; Klingstedt, M.; Dadachov, M. S.; O'Keeffe, M. *Nature* **2005**, *437*, 716. (c) Cheetham, A. K.; Férey, G.; Loiseau, T. *Angew. Chem., Int. Ed.* **1999**, *38*, 3268. (d) Suib, S. L. *Acc. Chem. Res.* **2008**, *41*, 479.

(12) (a) Cahill, C. L.; Ko, Y.; Parise, J. B. *Chem. Mater.* **1998**, *10*, 19–21. (b) Gao, J.; Tay, Q.; Li, P.-Z.; Xiong, W.-W.; Zhao, Y.; Chen, Z.; Zhang, Q. *Chem. - Asian J.* **2014**, *9*, 131–134.

(13) A mixture of S (0.032g), SnCl₂·2H₂O (0.067g), In(NO₃)₃ (0.090g), and 1,3-di(4-pyridyl)propane (dpp) (0.060g) in a molar ratio of 10:3:3:3 and ethanolamine (eta) (3 mL), H₂O (3 mL) in a 15-mL Teflon-lined stainless container and stirred for 0.5 h. The vessel was then sealed and heated to 160 °C for 7 days. After cooling to rt, the raw product was filtered off, washed with distilled water and ethanol, and further purified by the ultrasonic technique. The pale-yellow octahedral crystals were achieved with the yield of 25%. The deduced formula is [H₃O]₃[Heta]_{4.2}[H₂dpp]_{0.3} [In₄Sn₁₆O₁₀S₃₂]-33H₂O. The charge balance requires that there are three protonated water molecules in each formula.

(14) Crystal data for compound **1** tetragonal, *I*₄/acd, *a* = 23.1392(10) Å, *c* = 41.5631(19) Å, *V* = 22253.8(17) Å³, *Z* = 8, *D*_c = 2.116 g cm⁻³, *μ* = 4.948 mm⁻¹, *F*(000) = 12704.0, *R*₁ = 0.0444, *wR*₂ = 0.1056, *S* = 0.794.

(15) Slupecki, O.; Brown, I. D. *Acta Crystallogr., Sect. B: Struct. Crystallogr. Cryst. Chem.* **1982**, *38*, 1078.

(16) (a) Pauling, L. *The Nature Of The Chemical Bond And The Structure Of Molecules And Crystals; An Introduction To Modern Structural Chemistry* (3rd ed.). Cornell University Press, Ithaca (NY). 1960; pp 543–562. (b) Brown, I. D. *Chem. Rev.* **2009**, *109*, 6858–6919.

(17) (a) Albright, T. A.; Burdett, J. K.; Whangbo, M.-H. *Orbital Interactions in Chemistry*; Wiley: New York, 2013. (b) Bickelhaupt, F. M.; Baerends, E. J. *Rev. Comput. Chem.* **2000**, *15*, 1–86.